ACS APPLIED MATERIALS & INTERFACES

Research Article

www.acsami.org

Novel Amperometric Aptasensor Based on Analyte-Induced Suppression of Enzyme Catalysis in Polymeric Bionanocomposites

Yingchun Fu,*[,†] Can Zou,[†] Lijuan Bu,[†] Qingji Xie,*[,†] and Shouzhuo Yao[†,‡]

[†]Key Laboratory of Chemical Biology and Traditional Chinese Medicine Research (Ministry of Education), College of Chemistry and Chemical Engineering, Hunan Normal University, Changsha 410081, P. R. China

[‡]State Key Laboratory of Chemo/Biosensing and Chemometrics, College of Chemistry and Chemical Engineering, Hunan University, Changsha 410082, P. R. China

ABSTRACT: We report on a novel label-free biosensing interface based on multifunctional polymeric bionanocomposites (PBNCs) and its application for sensitive detection of protein based on the analyte-induced suppression of enzymatic catalysis in PBNCs. Thrombin and its aptamer are adopted as a model system to construct an amperometric aptasensor. First, polydopamine-based PBNCs with glucose oxidase (GOx) entrapped at high load/activity and Au nanoparticles (AuNPs) dispersed in high abundance on the surface were prepared through a chemical/biochemical synthesis method, as proven by UV−vis spectrophotometry, digital imaging, and transmission electron microscopy. Then, the PBNCs were cast-coated onto an Au electrode. The PBNC-modified Au electrode presented a high chronoamperometric sensitivity of 113 ± 2 μA cm^{-2} mM^{-1} to glucose, as well as a high capability of immobilizing the aptamer through the surficial AuNPs to fabricate a label-free aptasensing interface. The binding of thrombin to the aptasensor surface significantly hindered the mass-transfer of the enzymatic substrates/products and thus suppressed the enzymatic catalysis efficiency, which produced obvious signal change through measuring the electrooxidation of enzymatically generated H_2O_2. The thus-prepared aptasensor could detect thrombin with a broad detection range (1−100 nM), a detection limit down to 0.1 nM, and satisfactory specificity. The developed aptasensing method may find broad applications in the fields of clinical diagnosis, environmental protection, and food safety.

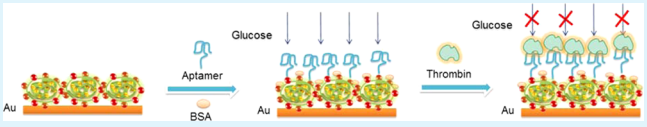

KEYWORDS: *label-free amperometric aptasensor, polymeric bionanocomposites, protein detection, enzymatic catalysis, thrombin*

INTRODUCTION

Sensitive and rapid detection of targets plays an increasingly important role in the fields of clinical diagnosis, environmental protection, and food safety. Biosensing, using bioprobes to sensitively and specifically capture targets and produce detectable signals, is regarded as one of the most powerful and promising tools to meet this end.[1] Generally, there are mainly two kinds of biosensing methods, namely, labeling one and label-free one. The labeling methods introduce functional species (labels) after the capture of analytes to efficiently produce/amplify signal, such as enzyme,[2,3] nanomaterials,[4,5] electroactive molecule.[6] However, this kind of method needs the conjugation of the biorecognition molecules with the labels directly or even indirectly using additional matrices, as well as additional incubation and/or signal readout procedures, which inevitably complicate the detection, increase the detection time, and lower reproducibility. In contrast, the label-free methods produce signals based on the electrochemical, optical, mass changes directly caused by the binding of the targets, which has shown high prospect for sensitive, fast, and simple detection of many analytes because of their simplicity, convenience, and low cost.[7−11] Obviously, the efficient immobilization of biorecognition molecules and the facile binding of analytes are two of the most essential properties of the label-free interface. Therefore, nanomaterials, electroactive molecules, and polymers are generally used to improve the label-free interface. As is well-known, enzymes exhibit strong catalysis ability but are susceptible to the surroundings, such as pH, temperature, and mass-transfer of substrates/products. Accordingly, enzymes are expected to be excellent candidates to construct sensitive label-free interface, however, such researches are rather limited.

Polymeric bionanocomposites (PBNCs) contain polymer, nanoparticles, biomolecules, and more components. The PBNCs can integrate the properties and functions of the individual components and even present intriguing synergy effects in some cases, thus they have shown great prospects for their obvious scientific and technical interests in various fields, especially in biosensing.[12] The polymer matrix with high processability and functionality is well-known to be capable of efficiently entrapping/adsorbing biomolecules[13−16] and nanoparticles,[17,18] endowing high abundance of biomolecules/nanomaterials in/on the PBNCs. The nanoparticles with significant adsorbability and biocompatibility can not only provide the PBNCs with abundant sites to bind biomolecules and retain the bioactivity,[13,19] but also endow the PBNCs with diversified functions for developing biodevices, including catalysis,[20,21] electronics,[15,16,22] optics,[23] and magnetics.[24] Additionally, the PBNCs are cost-effective, stable, and

Received: November 6, 2012
Accepted: December 26, 2012
Published: December 26, 2012

convenient in preparation. Virtually, our recent researches have demonstrated that the PBNCs based on polydopamine (PDA) can readily entrap glucose oxidase (GOx) at high load/activity and encapsulate/adsorb metal nanoparticles (Pt and Au nanoparticles, PtNPs and AuNPs). Accordingly, we have developed PBNC-based enzyme biosensor with a detection sensitivity as high as 129 μA cm^{-2} mM^{-1} to glucose,[16] as well as immunosensors with either the encapsulated/adsorbed PtNPs or GOx as labels, which could detect the target antigen down to pM.[14,15] In our opinion, the intriguing PBNCs with various functional species immobilized at high load/activity are expected to provide a new and promising platform for label-free aptasensing.

Herein, a novel label-free amperometric aptasensing method based on the suppression of enzymatic catalysis in PBNCs is developed for sensitive detection of protein. Thrombin and its aptamer are adopted as the model system for the aptasensor. As shown in Figure 1, the PBNCs are prepared using chemical synthesis and then biochemical synthesis, yielding PBNCs with GOx entrapped at high load/activity and AuNPs in high abundance on the surface. Some of the PBNCs are then cast-coated onto an Au electrode, and the aptamer is immobilized on the surficial AuNPs to fabricate the label-free aptasensor, as shown in Figure 2. The binding of thrombin to the immobilized aptamer can largely suppress the mass-transfer of the enzymatic substrates/products and thus the enzymatic reaction efficiency, leading to a notably decreased amperometric signal of electrooxidation of enzymatically produced H_2O_2.

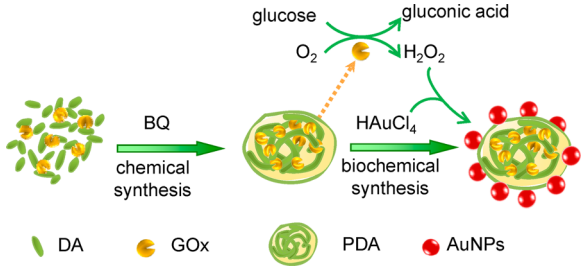

Figure 1. Illustration of the chemical/biochemical preparation of the PBNCs. DA, dopamine; BQ, benzoquinone.

MATERIALS AND APPARATUS

All electrochemical experiments were conducted on a CHI660C electrochemical workstation (CH Instruments Inc., Austin, TX), and a conventional three-electrode electrolytic cell was used. Au disk electrodes with 3.0-mm diameter (0.07 cm^2 area) served as the working electrode, a KCl-saturated calomel electrode (SCE) as the reference electrode, and a carbon rod as the counter electrode. All potentials here are cited versus SCE. The UV−vis spectra were recorded on a UV-2450 spectrophotometer (Shimazu, Japan). The transmission electron microscopy (TEM) image was collected on a JEM-1230 transmission electron microscope (JEOL, Japan).

Thrombin was purchased from Sigma. Thiolated thrombin aptamer of 25-base (TBA, 5′-SH-$(CH_2)_6$-$(T)_{10}$GGTTGGTGTGGTTGG-3′) was purchased from Sangon Co., Ltd. (Shanghai, China). Ten μM of TBA was prepared in 50 mM Tris buffer (pH 7.4, 140 mM NaCl, 5 mM KCl, 1 mM $MgCl_2$, 1 mM $CaCl_2$) and stored at −20 °C when not in use. GOx (EC 1.1.3.4; type II from *Aspergillus niger*, activity ≈ 150 kU g^{-1}) and dopamine (DA) were purchased from Sigma. Two kinds of PBS solutions, PBS **1** (pH 7.4, 0.10 M KH_2PO_4−K_2HPO_4 + 0.10 M K_2SO_4) and PBS **2** (10 mM NaH_2PO_4−Na_2HPO_4 + 0.15 M NaCl), were used for electrochemical and biorecognition experiments, respectively. All other chemicals were of analytical grade or better quality. Milli-Q ultrapure water (Millipore, ≥18 MΩ cm) was used throughout.

Preparation of Various PBNCs. As illustrated in Figure 1, the preparation of PBNCs involved the following procedures. First, 30 mM benzoquinone (BQ) was added into PBS **1** (0.1 mL) containing 30 mM DA and 4.0 mg mL^{-1} GOx, and this mixture was kept at 4 °C for 1 h to allow the chemical synthesis, yielding a suspension of the PDA−GOx bionanocomposites. Second, the suspension was centrifuged, and the yielded precipitates were then rinsed with PBS **2** three times and ultrasonically redispersed in PBS **2** (1.5 mL). Note that the formed AuNPs can be well dispersed in PBS **2** but poorly dispersed in PBS **1** of high-concentration ions (SO_4^{2-}). Third, 0.20 mM $HAuCl_4$ ($KAuCl_4$ at neutral pH instead) and 4.0 mM glucose (both final concentrations) were successively added into the yielded suspension to allow the biochemical synthesis, yielding a red suspension of the PDA-GOx-AuNPs PBNCs. When not in use, the prepared PBNCs were stored at 4 °C.

Fabrication and Characterization of Aptasensor. Bare Au electrode was cleaned according to the reported protocol.[25] Briefly, the Au electrode was carefully polished in 0.5 and 0.05 μm alumina suspensions in sequence. After thoroughly rinsed with water, the polished electrode was ultrasonically treated sequentially in water, ethanol, and water for 5 min each to remove residual alumina powder, respectively. Then, the Au electrode was treated with Piranha solution (H_2SO_4:H_2O_2, 3:1 in v/v, ***Caution:*** *highly oxidizing and corrosive, treat with great care*) for 15 s. Afterward, the Au electrode was subjected to electrochemical rinsing in 0.50 M H_2SO_4 to thoroughly remove impurities, namely, potentiostatic treatments at 2 V for 5 s and at −0.35 V for 10 s, and potential cycling for 6 cycles from −0.35 to 1.55 V at a scan rate of 4 V s^{-1}. The cleaned Au electrode was finally characterized by cyclic voltammetry (CV) from −0.35 to 1.55 V in 0.50 M H_2SO_4, which showed a single sharp reduction peak at ca. 0.9 V and multiple overlapping oxidation peaks at potentials ranging from 1.2 to 1.5 V.

The construction and characterization of the aptasensor are as follows. Before use, the PDA-GOx-AuNPs PBNCs were centrifuged again and dispersed in pure water, 1 μL of which was then casted onto the clean Au electrode surface and kept at 4 °C to form a PBNCs film after solvent evaporation (PBNCs/Au electrode). After rinse by Tris buffer, the PBNCs/Au electrode was immersed in the TBA solution for 16 h to complete the self-assembling of TBA on the AuNPs (TBA/PBNCs/Au). Afterward, the modified electrode was immersed in 1% BSA in Tris buffer for 1 h to block the nonspecific adsorption sites (BSA/TBA/PBNCs/Au). Finally, the aptasensors were incubated with thrombin in Tris buffer at different concentrations (thrombin/BSA/TBA/PBNCs/Au). After each step, the electrode was thoroughly washed by Tris buffer and then was characterized through the chronoamperometric response at 0.7 V to 2 mM glucose in stirred PBS

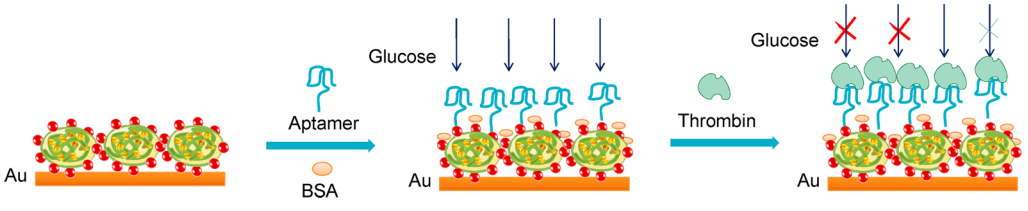

Figure 2. Illustration of the design and biosensing mechanism of the aptasensor.

dx.doi.org/10.1021/am302602s | ACS Appl. Mater. Interfaces 2013, 5, 934−939

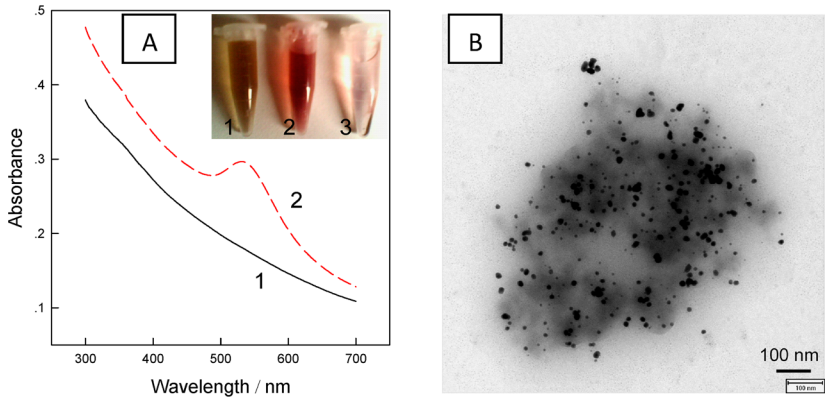

Figure 3. (A) UV−vis spectra and digital picture (inset) of (1) PDA-GOx nanocomposites and PBNCs (2) before and (3) after centrifugation. (B) TEM image of an individual PBNC.

1 solution. The response of the aptasensor to thrombin was collected through the change value of the potentiostatic responses before (BSA/TBA/PBNCs/Au) and after the incubation of thrombin (thrombin/BSA/TBA/PBNCs/Au).

The statistic analysis of data, including the mean and standard deviation, was conducted using Sigmaplot version 10 for Windows (Systat Software Inc., San Jose, CA) based on the results of at least three parallel experiments.

RESULTS AND DISCUSSION

Preparation and Characterization of the PBNCs. As shown in Figure 1, BQ was added into the mixture of DA and GOx to trigger the chemical synthesis, namely, BQ oxidized DA to form PDA, and lots of GOx were entrapped during formation of the PDA, yielding PDA-GOx nanocomposites. This method has been proven highly efficient to immobilize enzyme at high load/activity.[15,26] Then, glucose and $HAuCl_4$ were added into the PDA-GOx suspension to trigger the biochemical synthesis. The entrapped GOx catalyzed the oxidation of glucose and produced H_2O_2, which acted as a reductant to reduce $HAuCl_4$ into atomic Au. Aggregation of the yielded Au atoms formed AuNPs, many of which were then adsorbed onto the surface of PDA-GOx nanocomposites in proximity through the strong interaction between Au and the amino/imine groups in the PDA backbone, yielding PDA-GOx-AuNPs PBNCs. Because our previous study has proven that polydopamine is anion-repulsive,[16] so it should be hard for $AuCl_4^-$ anions to enter into the PBNCs to form AuNPs inside.

Digital pictures, UV−vis spectrophotometry, and TEM were adopted to monitor and characterize the preparation of the PDA-GOx composites and PBNCs. As shown in Figure 3, the PDA-GOx composites with blackish-brown color showed no absorption peak. However, the PBNCs suspension became red in color and showed obvious adsorption peak at ca. 530 nm, which is characteristic of the surficial plasma resonance of AuNPs.[14] The above data should prove the successful production of AuNPs. Furthermore, the PBNCs suspension was centrifuged at 5 krpm, yielding red precipitates and rather clear supernatant. This observation indicated that the produced AuNPs were dispersed on the surface of PBNCs through their strong interaction with PDA but not in the solution, because of the in situ reduction of $HAuCl_4$ by the enzymatically produced H_2O_2 in the proximity of PBNCs. The biochemical synthesis of AuNPs thus should benefit the large abundance of AuNPs on the PBNCs surface. TEM was also used to characterize the yielded PBNCs, as shown in Figure 3. An individual composite particle possesses at least 200 AuNPs of 5−25 nm diameter on its surface. The AuNPs with large surface-to-volume ratio and high abundance on the composite surface should be able to act as excellent capturing sites for TBA and the subsequent binding of the anchored TBA with thrombin.

Design and Construction of the Aptasensing Interface. The design and construction of the aptasensor is illustrated in Figure 2. First, the PBNCs have plenty of unoccupied amino/imide groups in the backbone of PDA on the surface, and these groups can bind to the Au electrode surface through the coordination interaction. On the other hand, the AuNPs and the amino/imide groups of the neighborhood PBNCs should have strong interaction to link to each other. Therefore, a firm and stable PBNCs film could be readily obtained using cast-coating method (PBNCs/Au). Then TBA can be immobilized on the PBNCs/Au electrode through the Au−S chemistry between plenty of exposed surface AuNPs of PBNCs and the thiol in TBA. After blocking of the nonspecific adsorption sites with BSA, the aptasensor highly specifically captured the target thrombin by forming G-quadruplex structure of aptamer to fit the binding site of thrombin.

CV using redox probes of $K_3[Fe(CN)_6]/K_4[Fe(CN)_6]$ is an effective way to probe the surface change of the electrode,[27] and CV was also used here to monitor and characterize the construction of the aptasensor. As shown in Figure 4, after the treatments of PBNCs, TBA, and BSA, the peak currents sharply decreased and the peak-to-peak potentials largely increased, indicating the successful modifications of the electrode, because the insulative and large-size PBNCs, TBA, and BSA could suppress the mass/electron-transfer of the redox probes to the electrode. Afterward, exposure of the aptasensor to 100 nM thrombin caused an additional large decrease of the redox current (even redox peaks disappeared). The findings highlight that the capture of thrombin on the aptasensor surface can largely hinder the mass/electron-transfer of redox probe, which inspires us to design a novel aptasensing method.

As is well-known, the enzymatic catalysis mainly depends on the enzymatic amount/activity and the accessibility/removability of the substrates/products. For the immobilized enzyme with their amount/activity kept constant in the matrix, the accessibility/removability of the substrates/products thus play key role on the enzymatic catalysis. For the enzymatic catalysis reaction of GOx entrapped in PBNCs on the electrode, the mass-transfer-in of the substrates of glucose and O_2, and the mass-transfer-away of the products of gluconic acid and H_2O_2,

dx.doi.org/10.1021/am302602s | ACS Appl. Mater. Interfaces 2013, 5, 934−939

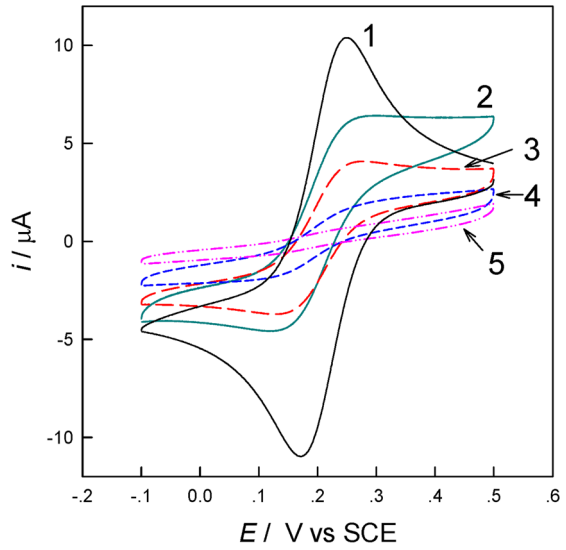

Figure 4. Cyclic voltammogramms at bare Au (curve 1), PBNCs/Au (curve 2), TBA/PBNCs/Au (curve 3), BSA/TBA/PBNCs/Au (curve 4), and thrombin/BSA/TBA/PBNCs/Au (curve 5) electrodes in PBS **1** (pH 7.0) containing 1.0 mM $K_3Fe(CN)_6$ + 1.0 mM $K_3Fe(CN)_6$. Scan rate: 100 mV s^{-1}.

should be very susceptive to the stuff-loading on the surface. This principle is elaborately utilized to design the novel label-free aptasensing interface here. To prove this concept, the enzyme catalysis efficiency of the aptasensor during the construction and detection was monitored through measuring the enzymatically produced H_2O_2 potentiostatically at 0.7 V, as shown in Figure 5. The PBNCs/Au electrode showed a rapid and large response to 2 mM glucose at a sensitivity of 113 ± 2 μA cm^{-2} mM^{-1}, which is obviously superior to those of other GOx-modified electrodes.[28−32] The high enzymatic catalysis efficiency should be due to the high enzymatic amount/activity of GOx in the PBNCs. The high sensitivity thus provided an interface with large capability to sense the stuff-loading

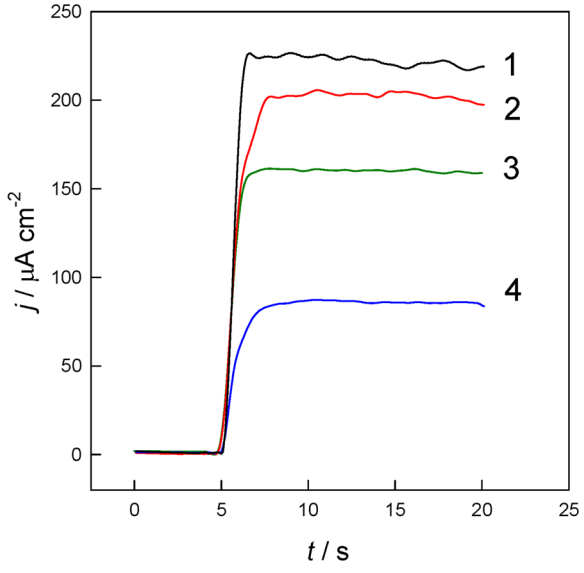

Figure 5. Chronoamperometric responses of PBNCs (curve 1), TBA/PBNCs (curve 2), BSA/TBA/PBNCs (curve 3), and thrombin/BSA/TBA/PBNCs (curve 4) modified Au electrodes in PBS **1** solution at 0.7 V to 2 mM glucose.

according to the suppression of the accessibility/removability of the substrates/products. As expected, after the modification/capture of TBA of a strand of 25 bases, the current response of the modified electrode decreased to 101 ± 2 μA cm^{-2} mM^{-1}, though the hindrance of H_2O_2 from diffusing away may increase the current response in some extent. This proved the successful modification of thiolated aptamer based on the AuNPs on the surface of PBNCs. The current responses to BSA and 100 nM thrombin decreased to 80 ± 2 and 42 ± 1 μA cm^{-2} mM^{-1}, which proved again the successful modifications as well as the feasibility and high sensitivity of the proposed aptasensing interface.

We also tested the effects of salt concentrations through changing the concentrations of K_2SO_4 in PBS 1 during the detection using thrombin/BSA/TBA/PBNCs/Au electrodes, as shown in Figure 6A. We found that the responses kept increasing till the concentration of K_2SO_4 increased to 0.1 M and then kept constant. This should indicate that 0.1 M K_2SO_4 was necessary for the enzymatic catalysis and electrochemical detection. We also investigated how the acidity affected the response through conducting the detections of 2 mM glucose in PBS solutions with pH range from 5.2 to 7.4 using BSA/TBA/PBNCs/Au electrodes (blue curve) and thrombin/BSA/TBA/PBNCs/Au electrodes (red curve), as shown in Figure 6B. For convenience, we used the percentages of responses at different pH values to that at pH 7.4. Generally, we found the lower the pH value, the lower the response in both two cases, as a result of the suppression of the enzymatic catalysis in acidic surroundings. Interestingly, at pH range from 5.6 to 7, the responses after the binding of thrombin were larger than that before the binding, this might be due to that some bound thrombin were detached in acidic surroundings and increased the response. In PBS solutions with pH lower than 5.6, the low enzymatic activity should dominate the low response in both cases, so those responses were very similar.

Performance and Evaluation of the Aptasensor. On the basis of the suppression of the enzymatic catalysis by the target, the proposed aptasensor was applied to amperometrically detect thrombin, as shown in Figure 7. The signal is picked as the change between the potentiostatic amperometric response before (BSA/TBA/PBNCs/Au electrode) and after (thrombin/BSA/TBA/PBNCs/Au electrode) the incubation of thrombin. The aptasensor presented successive decreases of current to the increase of thrombin concentration, and the response time at each concentration was less than 5 s. The broad linear range from 1 to 100 nM and the detection limit down to 0.1 nM (S/N = 3) are comparable to or better than other analogues.[33−39] Here, the following reasons should contribute to the satisfactory aptasensing response. (1) The highly efficient immobilization of enzyme in the PBNCs made the PBNCs/Au electrode a good platform to sensitively response thrombin-loading. (2) The PBNCs with high surface-abundance of AuNPs provided efficient matrix for immobilization of TBA to efficiently bind thrombin. (3) The novel aptasensing method based on the high susceptibility of GOx to mass-transfer of substrates/products (suppression of enzymatic catalysis) endowed sensitive response to the thrombin capture.

Since the PBNCs and the AuNPs on their surface endow plenty of immobilization sites for TBA, the possible nonspecific adsorption on these sites was also investigated. The PBNCs/Au electrode was blocked with BSA (without prior binding of TBA) and then exposed to 100 nM thrombin. The current

dx.doi.org/10.1021/am302602s | ACS Appl. Mater. Interfaces 2013, 5, 934−939

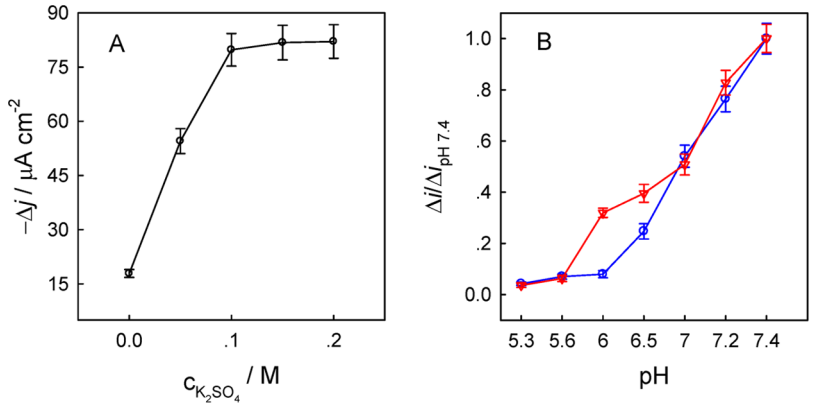

Figure 6. (A) Response of the thrombin/BSA/TBA/PBNCs/Au electrodes in PBS solutions with different concentrations of K_2SO_4 at 0.7 V to 2 mM glucose. (B) The percentages of the responses of the BSA/TBA/PBNCs/Au electrodes (blue curve) and thrombin/BSA/TBA/PBNCs/Au electrodes (red curve) in PBS solutions at different acidity to that at pH 7.4, detection potential: 0.7 V.

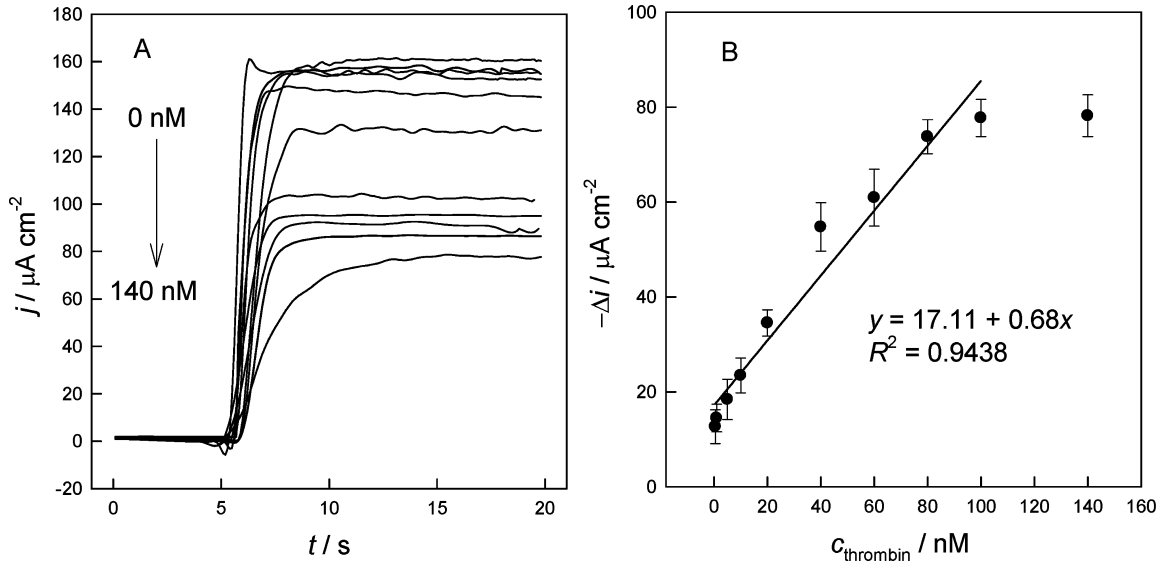

Figure 7. (A) Chronoamperometric responses of the aptasensors incubated with thrombin at various concentrations in PBS **1** at 0.7 V to 2 mM glucose. (B) Calibration curve of the aptasensor.

response change was just 0.65% (n = 3) of that when using TBA (BSA/TBA/PBNCs/Au electrode), indicating very minor nonspecific adsorption of thrombin on the electrode surface after the BSA blocking.

The specificity of the aptasensor against some other common proteins was also investigated. The aptasensors were exposed to BSA, human serum albumin (HSA), immunoglobulin G (IgG), and fibrinogen each at concentration of 10 μM, respectively, then the current response changes were recorded, as shown in Figure 8. The responses of the aptasensor to these proteins were all less than 8% (n = 3) of that for 100 nM thrombin even their concentrations were 100-fold higher. This should prove that the proposed aptasensor has satisfactory specificity.

CONCLUSIONS

A novel amperometric aptasensing interface has been developed based on the PBNCs materials modified electrode and the analyte-induced suppression of enzymatic catalysis. The PBNC-modified electrode with GOx entrapped at high load/activity provided a good platform with high sensitivity to sense the thrombin-loading. The susceptibility of enzyme catalysis to the mass-transfer of enzymatic substrates/products endowed

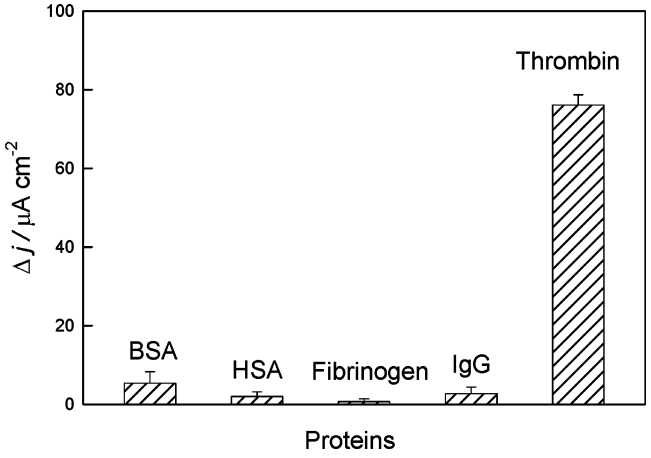

Figure 8. Response changes of the aptasensor in PBS 1 solution at 0.7 V to 2 mM glucose, before and after incubation with 10 mM BSA, HSA, fibrinogen, IgG antibody, and 100 nM thrombin, respectively.

the aptasensor high detection sensitivity to thrombin with a detection limit down to 0.1 nM, which is comparable to or

dx.doi.org/10.1021/am302602s | ACS Appl. Mater. Interfaces 2013, 5, 934−939

better than that of analogues. The aptasensor also presented a broad linear detection range, rapid response time, and satisfactory specificity. The proposed concept based on the suppression of enzyme catalysis may open new avenues for other aptasensing, immunosensing, and biocatalysis applications.

AUTHOR INFORMATION

Corresponding Author

*E-mail: yingchunfu@126.com (Y.F.); xiegj@hunnu.edu.cn (Q.X.).

Notes

The authors declare no competing financial interest.

ACKNOWLEDGMENTS

This work was supported by the National Natural Science Foundation of China (Grants 21075036, 21175042, 21105026, 20875029), the Foundations of Hunan Provincial Education Department (11A069, 11B078) and Hunan Province (Grant 11JJ4014), Specialized Research Fund for the Doctoral Program of Higher Education (20114306120004), Program for Science and Technology Innovative Research Team in Higher Educational Institutions of Hunan Province, Hunan Lotus Scholars Program, and State Key Laboratories of Chemo/Biosensing and Chemometrics (Grants 200902, 201104) and of Electroanalytical Chemistry.

REFERENCES

(1) Lei, J.; Ju, H. *Chem. Soc. Rev.* **2012**, *41*, 2122−2134.
(2) Liu, B.; Zhang, B.; Cui, Y.; Chen, H.; Gao, Z.; Tang, D. *ACS Appl. Mater. Interfaces* **2011**, *3*, 4668−4676.
(3) Li, Q.; Zeng, L.; Wang, J.; Tang, D.; Liu, B.; Chen, G.; Wei, M. *ACS Appl. Mater. Interfaces* **2011**, *3*, 1366−1373.
(4) Baeissa, A.; Dave, N.; Smith, B. D.; Liu, J. *ACS Appl. Mater. Interfaces* **2010**, *2*, 3594−3600.
(5) Shukoor, M. I.; Altman, M. O.; Han, D.; Bayrac, A. T.; Ocsoy, I.; Zhu, Z.; Tan, W. *ACS Appl. Mater. Interfaces* **2012**, *4*, 3007−3011.
(6) Fu, Y.; Wang, T.; Bu, L.; Xie, Q.; Li, P.; Chen, J.; Yao, S. *Chem. Commun.* **2011**, *47*, 2637−2639.
(7) Sorgenfrei, S.; Chiu, C.-y.; Gonzalez, R. L.; Yu, Y.-J.; Kim, P.; Nuckolls, C.; Shepard, K. L. *Nat. Nano.* **2011**, *6*, 126−132.
(8) Du, Y.; Chen, C.; Yin, J.; Li, B.; Zhou, M.; Dong, S.; Wang, E. *Anal. Chem.* **2010**, *82*, 1556−1563.
(9) Chu, P.-T.; Lin, C.-S.; Chen, W.-J.; Chen, C.-F.; Wen, H.-W. *J. Agric. Food Chem.* **2012**, *60*, 6483−6492.
(10) Papadakis, G.; Tsortos, A.; Bender, F.; Ferapontova, E. E.; Gizeli, E. *Anal. Chem.* **2012**, *84*, 1854−1861.
(11) Ly, N.; Foley, K.; Tao, N. *Anal. Chem.* **2007**, *79*, 2546−2551.
(12) Bitinis, N.; Hernandez, M.; Verdejo, R.; Kenny, J. M.; Lopez-Manchado, M. A. *Adv. Mater.* **2011**, *23*, 5229−5236.
(13) Liu, Y. G.; Feng, X. M.; Shen, J. M.; Zhu, J. J.; Hou, W. H. *J. Phys. Chem. B* **2008**, *112*, 9237−9242.
(14) Fu, Y.; Li, P.; Bu, L.; Wang, T.; Xie, Q.; Xu, X.; Lei, L.; Zou, C.; Yao, S. *J. Phys. Chem. C* **2010**, *114*, 1472−1480.
(15) Fu, Y.; Li, P.; Wang, T.; Bu, L.; Xie, Q.; Xu, X.; Lei, L.; Zou, C.; Chen, J.; Yao, S. *Biosens. Bioelectron.* **2010**, *25*, 1699−1704.
(16) Fu, Y.; Li, P.; Xie, Q.; Xu, X.; Lei, L.; Chen, C.; Zou, C.; Deng, W.; Yao, S. *Adv. Funct. Mater.* **2009**, *19*, 1784−1791.
(17) Li, D. X.; He, Q.; Cui, Y.; Wang, K. W.; Zhang, X. M.; Li, J. B. *Chem.—Eur. J.* **2007**, *13*, 2224−2229.
(18) Liu, Z.; Wang, J.; Xie, D.; Chen, G. *Small* **2008**, *4*, 462−466.
(19) Yan, W.; Chen, X. J.; Li, X. H.; Feng, X. M.; Zhu, J. J. *J. Phys. Chem. B* **2008**, *112*, 1275−1281.
(20) Luo, X. L.; Killard, A. J.; Smyth, M. R. *Chem.—Eur. J.* **2007**, *13*, 2138−2143.
(21) Granot, E.; Katz, E.; Basnar, B.; Willner, I. *Chem. Mater.* **2005**, *17*, 4600−4609.
(22) Shen, Y.; Lin, Y. H.; Nan, C. W. *Adv. Funct. Mater.* **2007**, *17*, 2405−2410.
(23) Ventura, M. J.; Gu, M. *Adv. Mater.* **2008**, *20*, 1329−1332.
(24) Shokouhimehr, M.; Piao, Y.; Kim, J.; Jang, Y.; Hyeon, T. *Angew. Chem., Int. Ed.* **2007**, *46*, 7039−7043.
(25) Zhang, J.; Song, S. P.; Wang, L. H.; Pan, D.; Fan, C. H. *Nat. Protoc.* **2007**, *2*, 2888−2895.
(26) Fu, Y.; Chen, C.; Xie, Q.; Xu, X.; Zou, C.; Zhou, Q.; Tan, L.; Tang, H.; Zhang, Y.; Yao, S. *Anal. Chem.* **2008**, *80*, 5829−5838.
(27) Srivastava, R. K.; Srivastava, S.; Narayanan, T. N.; Mahlotra, B. D.; Vajtai, R.; Ajayan, P. M.; Srivastava, A. *ACS Nano* **2012**, *6*, 168−175.
(28) Wu, J.; Yin, L. *ACS Appl. Mater. Interfaces* **2011**, *3*, 4354−4362.
(29) Muguruma, H.; Hoshino, T.; Matsui, Y. *ACS Appl. Mater. Interfaces* **2011**, *3*, 2445−2450.
(30) Luo, X. L.; Xu, J. J.; Wang, J. L.; Chen, H. Y. *Chem. Commun.* **2005**, *16*, 2169−2171.
(31) Cosnier, S.; Stoytcheva, M.; Senillou, A.; Perrot, H.; Furriel, R. P. M.; Leone, F. A. *Anal. Chem.* **1999**, *71*, 3692−3697.
(32) McMahon, C. P.; Rocchitta, G.; Serra, P. A.; Kirwan, S. M.; Lowry, J. P.; O'Neill, R. D. *Anal. Chem.* **2006**, *78*, 2352−2359.
(33) Radi, A.-E.; Sánchez, J. L. A.; Baldrich, E.; O'Sullivan, C. K. *J. Am. Chem. Soc.* **2006**, *128*, 117−124.
(34) Polsky, R.; Gill, R.; Kaganovsky, L.; Willner, I. *Anal. Chem.* **2006**, *78*, 2268−2271.
(35) Nutiu, R.; Li, Y. *J. Am. Chem. Soc.* **2003**, *125*, 4771−4778.
(36) Li, B.; Wei, H.; Dong, S. *Chem. Commun.* **2007**, 73−75.
(37) Pavlov, V.; Xiao, Y.; Shlyahovsky, B.; Willner, I. *J. Am. Chem. Soc.* **2004**, *126*, 11768−11769.
(38) Wei, H.; Li, B.; Li, J.; Wang, E.; Dong, S. *Chem. Commun.* **2007**, 3735−3737.
(39) Wang, Y.; Liu, B. *Langmuir* **2009**, *25*, 12787−12793.